Technology in Cancer Research & Treatment
Volume 22: 1-12

DOI: 10.1177/15330338231177807
journals.sagepub.com/home/tct

LHPP Inhibits the Viability, Migration, and Proliferation of PDAC Cells and Significantly Affects the Expression of SDC1 and S100p

Zhaozhi Xia, MM[1], Shuchao Zhao, MM[1], Xin Gao, MM[1], Hongrui Sun, MM[1], Faji Yang, MD[1], Huaqiang Zhu, MD[1], Hengjun Gao, MD[1], Jun Lu, MD[1], and Xu Zhou, MD[1]

Abstract

Introduction: Pancreatic ductal adenocarcinoma (PDAC) is a highly aggressive malignancy with a poor response to chemotherapy and an extremely poor prognosis. Recent studies have revealed that phospholysine phosphohistidine inorganic pyrophosphate phosphatase (LHPP) can inhibit the growth of various cancers. Therefore, the current study was conducted to investigate the antitumor effects of LHPP in PDAC and to explore its mechanism using proteomics analysis. **Methods and Results:** Immunohistochemical analysis of clinical samples demonstrated that LHPP expression levels were lower in tumor tissues compared to adjacent nontumor tissues. Moreover, multivariate COX regression analysis showed that LHPP expression level was an independent prognostic factor for the patients with PDAC. Patients with high LHPP expression had a better prognosis. The lentiviral vectors for normal control (NC), *LHPP* knockdown (KD), and *LHPP* overexpression (OE) were infected with BxPC-3 and PANC-1 cell lines. Cell counting kit-8 assay, Transwell assay, and flow cytometry analyses showed that LHPP overexpression significantly inhibited the cell viability, migration, and proliferation of BxPC-3 and PANC-1 cells. Moreover, xenograft tumor model demonstrated that LHPP overexpression inhibited xenograft tumor growth *in vivo*. Subsequently, proteins with significantly altered expression in BxPC-3 cells after lentivirus infection were detected using proteomics analyses. Interestingly, compared to the NC group, the expression of Syndecan 1 (SDC1) was significantly upregulated in the KD group, while that of S100P was significantly downregulated in the OE group. **Conclusion:** LHPP might emerge as an important target for delaying the advancement of PDAC, thereby providing a novel therapeutic approach for the treatment of PDAC.

Keywords

pancreatic ductal adenocarcinoma, LHPP, SDC1, S100P, proteomics

Abbreviations

AJCC, American Joint Committee on Cancer; CCK-8, cell counting kit-8 assay; CI, confidence interval; DAB, diaminobenzidine; EMT, epithelial-to-mesenchymal transition; GO, gene ontology; HCC, hepatocellular carcinoma; HR, hazard ratio; HSPG, heparin sulfate proteoglycan; IHC, immunohistochemical; KEGG, Kyoto Encyclopedia of Genes and Genomes; LHPP, phospholysine phosphohistidine inorganic pyrophosphate phosphatase; PDAC, pancreatic ductal adenocarcinoma; PI3K, phosphatidylinositol 3 kinase; PRM, parallel reaction monitoring; RT-qPCR, real-time quantitative polymerase chain reaction; S100P, S100 calcium-binding protein P; SDC1, Syndecan 1; SPSS, Statistical Product Service Solutions; TMT, tandem mass tag; TNM, tumor node metastasis; WB, western blot.

Received: October 27, 2022; Revised: April 28, 2023; Accepted: May 8, 2023.

Introduction

Pancreatic ductal adenocarcinoma (PDAC) is a highly aggressive malignancy, the incidence of which is increasing annually.[1] PDAC lacks early clinical symptoms, and most (80%-85%)

[1] Department of Hepatobiliary Surgery, Shandong Provincial Hospital Affiliated to Shandong First Medical University, Jinan, China

Corresponding Author:
Xu Zhou, MD, Department of Hepatobiliary Surgery, Shandong Provincial Hospital Affiliated to Shandong First Medical University, No. 324, Jingwuweiqi Road, Huaiyin District, China.
Email: zhouxu2008@sina.com

patients are diagnosed with invasion of cancer cells into adjacent tissues or organs, thereby losing the chance of radical cure, with a 5-year survival rate of 2% to 9%.[2,3] PDAC is not sensitive to chemotherapy, and survival for patients who receive chemotherapy is only a few months to half a year. Recent studies showed several prognostic factors for PDAC to guide the treatment strategy for PDAC. However, the clinical application is limited due to suboptimal specificity and sensitivity.[4-6] Therefore, it is essential to explore new effective PDAC therapeutic targets and prognostic factors to adjust the treatment strategy for PDAC.

Protein phosphatases play a critical role in cellular signaling pathways, and their dysregulated expression is significantly involved in cancer development.[7] Phospholysine phosphohistidine inorganic pyrophosphate phosphatase (LHPP) was originally identified in swine brain tissue.[8] A study in patients with hepatocellular carcinoma (HCC) identified LHPP as a potential tumor suppressor, and its dysregulated expression contributed to the development of HCC.[9] Subsequent studies have also suggested that LHPP can inhibit cervical cancer, papillary thyroid cancer, bladder cancer, and colorectal cancer via the phosphatidylinositol 3 kinase (PI3K)/AKT pathway.[10-13]

The current study first analyzed the data from clinical samples to assess the relevance of LHPP levels to the prognosis of patients with PDAC. Subsequently, *in vivo* and *in vitro* experiments were used to validate the antitumor effects of LHPP in PDAC cells. Finally, proteomic analysis using tandem mass tag (TMT) and parallel reaction monitoring (PRM) was performed to identify differentially expressed proteins affected by LHPP to explore its anticancer mechanisms.

Materials and Methods

Patients and Samples

Clinicopathological data and pathological tissue wax blocks were collected from patients with PDAC who underwent surgical treatment at the Department of Hepatobiliary Surgery, Shandong Provincial Hospital affiliated to Shandong First Medical University, from September 2004 to December 2008. The criteria for patients included in this study were as follows: (1) age between 18 and 90 years; (2) no preoperative radiotherapy, chemotherapy, or neoadjuvant therapy; and (3) PDAC diagnosed by pathology. The following criteria were used to exclude patients: (1) incomplete clinicopathological data or pathological tissue wax blocks; (2) incomplete follow up; and (3) had received postoperative radiotherapy, chemotherapy, or neoadjuvant therapy. Based on these criteria, a total of 99 patients were enrolled in this study. Clinical data including: gender, age, tumor location, pathological grade, tumor node metastasis classification, American Joint Committee on Cancer staging, short-time postoperative death, and survival time, were collected from an out-patient clinic or (and) follow up on the telephone. Survival time of <6 months was considered as short-term survival.

The human tissue samples involved and the associated experimental plan in this study were approved by the Ethics Committee of Shandong Provincial Hospital (2020-3019; dated: December 19, 2020), and written informed consent was obtained from all included patients. The patient consented to the collection of tissue, its use in the experiments, and the publication of the results. The patients were informed about the purpose and main content of the whole study. This study does not involve any patient privacy.

Immunohistochemical Staining

Tissue wax blocks were serially cut into 4 μm thick sections, and the tissue sections were routinely deparaffinized and hydrated. Hydrogen peroxide was used to inactivate peroxidase. Samples were incubated overnight at 4 °C with LHPP primary antibody (sc-376527), and then incubated with the goat-antirabbit secondary antibody (#7076, Cell Signaling Technology). Color development was performed with diaminobenzidine, and the nuclei were counterstained using hematoxylin. Three pathologists, who did not access to the patient's data, independently read and scored the immunohistochemical (IHC) staining results. The presence of brown granules in the cytoplasm was considered a positive result. The staining intensities of negative, weakly positive, moderately positive, and strong positive were scored as 0, 1, 2, and 3 points, respectively. The value >1 indicated high expression of LHPP, while the value ≤1 suggested low expression of LHPP.

Cells Culture

Human PDAC cell lines (BxPC-3 and PANC-1) were purchased from Shanghai Genechem Co., Ltd. PANC-1 and BxPC-3 cells were cultured in DMEM (10-013-CVR, Corning) and RPM1-1640 cell culture medium (15-059-CVR, Corning), respectively, containing 10% fetal bovine serum (FBS, VS500 T, A11-102, Ausbian).

Lentiviral Infection

LV-LHPP (42862-1) lentivirus, LV-LHPP-RNAi (81742-1) lentivirus, and negative control lentivirus (CON313) were purchased from Shanghai Genechem Co., Ltd. The target sequence of LHPP was 5′-CAACCCAAACTGTGTGGTAAT-3′. BxPC-3 and PANC-1 cells were infected with negative control lentivirus (NC group), *LHPP*-knockdown lentivirus (KD group), and *LHPP*-overexpressing lentivirus (OE group), respectively, according to the manufacturer's instructions. And 72 h later, the expression levels of LHPP were observed by fluorescence microscope to ensure an infection efficiency of 80% or more.

Real-Time Quantitative Polymerase Chain Reaction Analysis

TRIzol reagent (3101-100, Shanghai Pufei Biotechnology Co., Ltd) was used to isolate and extract total RNA. The concentration and quality of the extracted RNA were determined using a nanodrop spectrophotometer (Thermo). Complementary DNA

(cDNA) was synthesized using a cDNA synthesis kit (TaKaRa, Japan). Real-time quantitative polymerase chain reaction (RT-qPCR) analysis was performed using an SYBR Master mix (DRR041B, TaKaRa) and an RT-qPCR instrument (LightCycler 480 II, Roche). The primer sequences were as follows: LHPP-F: 5'-GCCAGATCCTGAAGGAGCAA-3', *LHPP*-R: 5'-GAGCACCTGGAAGGCGTTAT-3', GAPDH-F: 5'-TGACTTCAACAGCGACACCCA-3', and GAPDH-R: 5'-CACCCTGTTGCTGTAGCCAAA-3'.

Western Blot Analysis

Total proteins were extracted using radio immunoprecipitation assay lysis buffer (P0013B/, Beyotime). Protein contents were determined using a bicinchoninic acid (BCA) protein sequencing kit (P0010S/, Beyotime). Then, SDS-PAGE (sodium dodecyl sulfate-polyacrylamide gel electrophoresis; VE-180, Tanon) was performed. The proteins were transferred to the PVDF membrane (IPVH00010, Millipore) by electroporation at 4 °C with a constant current of 300 mA for 150 min. PVDF membrane was blocked by incubating with 6% nonfat milk at room temperature for 1.5 h. The blocked PVDF membrane was first incubated with primary antibody for 2 h at room temperature, and then incubated with secondary antibody for 1.5 h. Information on the antibodies used in this study was as follows: anti-LHPP (ab254788, 1:1000, Abcam), anti-β-actin (ab8226, 1:5000, Abcam), anti-SDC1 (10593-1-AP, 1:2000, Proteintech), and anti-S100P (11803-1-AP, 1:2000, Proteintech). The membrane was then removed after incubation. ECL-PLUS/Kit luminescent solution (Thermo) was added and exposed on a chemical colorimeter (4600, Tanon) for 1 s to several minutes. The exposure time was adjusted according to the visual observation of the fluorescence.

Cell Proliferation Assay

Cell Counting Kit-8 (CCK-8, Dojindo Chemical Laboratory) was used to detect cell viability. The cell density was set to 2500 cells/well, and inoculated into 96-well plates. Each well was injected with 100 μL serum-free medium (n = 3 wells per each group) for 5 days. Starting on day 2 after inoculation, 10 μL CCK-8 reagent was added to the wells 2 h before the termination of culture, and incubated continuously for 4 h. The plates were then placed on a shaker for 2 min, and the optical density $(OD)_{450}$ of each well was measured using a microplate reader (M2009PR, Tecan infinite).

Cell Migration Assay

Cell migration capacity was assessed using an 8 m Transwell chamber (7534, Corning). First, 100 μL serum-free media was added to the upper chamber and incubated for 1.5 h at 37 °C. Then, 550 μL of medium containing 30% FBS and 150 μL of cell suspension were added to the lower and upper chambers, respectively, and incubated for 24 h. The migrated cells were fixed with 4% paraformaldehyde fixative solution (Sinopharm Chemical Reagent Co., Ltd) for 30 min, and stained with crystal violet (R20755, Shanghai yuanye Bio-Technology Co., Ltd) for 5 min. Under the microscope, the field view was randomly selected, and 6 images at 100X and 12 images at 200X were taken. The images taken at 200X were used for data analysis and cell counting to assess the differences between the cell migration abilities of the experimental and control groups.

Flow Cytometry

When cells reached 80% cell confluency on 6-cm well plates, they were digested with trypsin and collect with complete medium in a 5 mL centrifuge tube. Cell was centrifuged at 4°C and 1200 rpm for 5 min. After centrifugation, they were washed once with precooled D-Hanks (pH = 7.4, Shanghai Genechem Co., Ltd) solution. Cells were fixed with 75% precooled ethanol (precooled at 4 °C for at least an hour). The fixative solution was then removed, and the cells were washed again with D-Hanks solution. The 40×PI (2 mg/mL) and 100×RNase stock solutions (10 mg/mL) were prepared into 1× cell staining solution using 1×D Hanks. Onboard testing and data were analyzed.

Xenograft Tumor Model

BxPC-3 cells (5×10^6 cells/mice) from the NC, KD, and OE groups were injected into the right underarm skin of BALB/c nude mice (4 weeks old, female) (Shanghai Lingchang Biotechnology Co., Ltd) (6 mice per group, random assignment). On the third day of injection, the body weight of the nude mice and the width and height of the tumor masses formed under the skin were measured, followed by twice weekly measurements to detect the volume of the tumor masses and to draw volume curves. Mice were euthanized on the 34th day of injection. Three mice were placed in the container at a time, and air was first provided, followed by a gradual increase in CO_2 concentration until respiratory cardiac arrest occurred. The CO_2 replacement rate was 40% of the container volume per minute. Tumor tissues were isolated, weighed, and photographed. Efforts were made in this study to reduce the number of animals used and to reduce their suffering. No other agents were used in this study. The reporting of this study conforms to ARRIVE 2.0 guidelines.[14] This study followed the 'Guide for the Care and Use of Laboratory Animals, 8th Edition'.[15] The animal-related experimental plan involved in this study was approved by the Ethics Committee of Shanghai Genechem Co. Ltd (GSZE0257693; dated: October 27, 2020).

TMT Quantitative Proteomic Analysis

An appropriate amount of SDT lysis buffer was added to the infected BxPC-3 cells and incubated in boiling water for 15 min. The samples were then centrifuged at 14,000 *g* for 15 min, and the supernatant was collected. Total protein

content was determined by BCA analysis. After adding 6X loading buffer to each 20 μg protein sample, they were incubated in boiling water for 5 min. Samples were run on 12% SDS-PAGE at a constant voltage of 250 V for 40 min, followed by staining with Coomassie brilliant blue. Then, the proteins were digested into peptide fragments using FASP enzymatic hydrolysis. And 100 μg of peptide fragments were taken from each sample and labeled using a TMT labeling kit (Thermo) according to the manufacturer's instructions. The labeled peptides from each group were pooled and fractionated using an Agilent 1260 infinity II HPLC system. The Nanoliter flow Easy nLC system was used to separate each sample. Solution A was 0.1% formic acid aqueous solution, and solution B was 0.1% formic acid acetonitrile aqueous solution (acetonitrile is 80%). The chromatographic column (Thermo Fisher Scientific, Acclaim PepMap RSLC 50 μm X 15 cm, nano viper, P/N164943) was calibrated using 100% solution A. The sample was loaded from the autosampler onto the analytical column, and the sample components were separated at a flow rate of 300 nL/min. The samples were chromatographed and analyzed using a Q Exactive Plus mass spectrometer. The parameters used in the mass spectrometry analysis were as follow: the analysis time was 90 min; the detection mode was positive ion; the precursor ion scanning range was 350 to 1800 m/z; the resolution of the primary mass spectrometer was 70,000; the AGC target was 3e6; and the maximum IT of the primary ion was 50 ms. A total of 10 fragment maps (MS2 scan) were collected after each full scan. The secondary spectrum acquisition parameters were as follows: the MS2 activation type was HCD; the isolation window was 2 m/z; the MS2 resolution was 35,000; the AGC target was 2e5; the minimum AGC target was 2e3; the secondary maximum IT was 45 ms; the collection charge was 2 to 6; the ion dynamic exclusion time was 30 s; and the normalized collision energy was 30 eV. A high-resolution mass spectrometer Q Exactive Plus for TMT quantitative proteomic analysis was used in this study. Library identification and quantitative analysis were performed using Mascot2.6 and Proteome Discoverer2.2 software, and the database used in this study was Uniprot_HomoSapiens_20367_20200226 (download link: http://www.uniprot.org). The proteins with Fold Change (FC) > 1.2 and *P*-value (Student's *t*-test) <.05 were considered to have significant differential expression.

Bioinformatics Analysis

Protein expression levels of LHPP in several malignant tumors and normal tissues were obtained from UALCAN (https://ualcan.path.uab.edu/).[16] Protein functional enrichment was performed using gene ontology (GO)[17] and pathway enrichment analysis. Pathway enrichment analysis was performed using the KEGG (Kyoto Encyclopedia of Genes and Genomes) database.[18] Fisher's exact test was used for target protein enrichment analysis.

PRM-MS Analysis

A 2 μg sample was injected and separated using nano-LC, followed by an online electrospray tandem mass spectrometry analysis. The complete LC-MS set consisted of a liquid phase system (Easy nLC system, Thermo Fisher Scientific) and a mass spectrometry system (Q-Exactive Plus, Thermo Fisher Scientific). Solution A and B were 0.1% formic acid in water and 0.1% formic acid in acetonitrile in water (80% in acetonitrile). Sample was separated using a nonlinearly growing gradient solution in an analytical column (Thermo Fisher Scientific, Acclaim PepMap RSLC 50 μm × 15 cm, nano viper, P/N164943) at a flow rate of 300 nL/min. LC cycle conditions were as follows: 0 to 1 min, the linear gradient of solution B increased from 2% to 8%; 1 to 46 min, the linear gradient of solution B increased from 8% to 28%; 46 to 56 min, the linear gradient of solution B increased from 28% to 40%; 56 to 57 min, the linear gradient of solution B increased from 40% to 90%; 57 to 60 min, the linear gradient of solution B maintained at 90%. The MS parameters were set as follows: the scan range (m/z) was 350 to 1500; the resolution was 60,000; the AGC target was 1e6; and the maximum injection time was 50 ms. For PRM, the resolution was 15,000, the AGC target was 1e5, the maximum injection time was 50 ms, the loop count was 10, the isolation window was 1.6 m/z, and the NCE was 27%.

Statistical Analyses

All statistical analyses were performed using Statistical Product Service Solutions 22.0 (IBM Corporation). Categorical carriable data in the basic biological characteristics, baseline graph, and effect determination were used for Pearson's chi-square test and continuity-corrected chi-square test, which were expressed as the χ^2 test. Continuous variables with a normal distribution were expressed as means and standard deviation (SD) of the mean. Kaplan-Meier survival analysis was performed, and the survival curves were drawn using GraphPad Prism 6.0. Most experiments were performed in triplicates. *P*-value <.05 was considered statistically significant.

Results

High Expression of LHPP is Associated With Better Clinical Outcomes in Patients With PDAC

Analysis of data covered by the the cancer genome atlas and clinical proteome tumor analysis consortium databases showed reduced expression of LHPP in most types of tumors, including PDAC, as shown in Figure 1a and b. The results were verified by IHC experiments performed on tumor tissues (n = 99) and adjacent nontumor tissues (n = 71) collected clinically from patients with PDAC. The IHC results confirmed that LHPP expression levels were decreased in PDAC tissues (*P* = .001), as shown in Figure 1c and d. Based on the expression level of LHPP, patients were divided into 2 groups, including the LHPP high expression group (n = 35 patients) and the

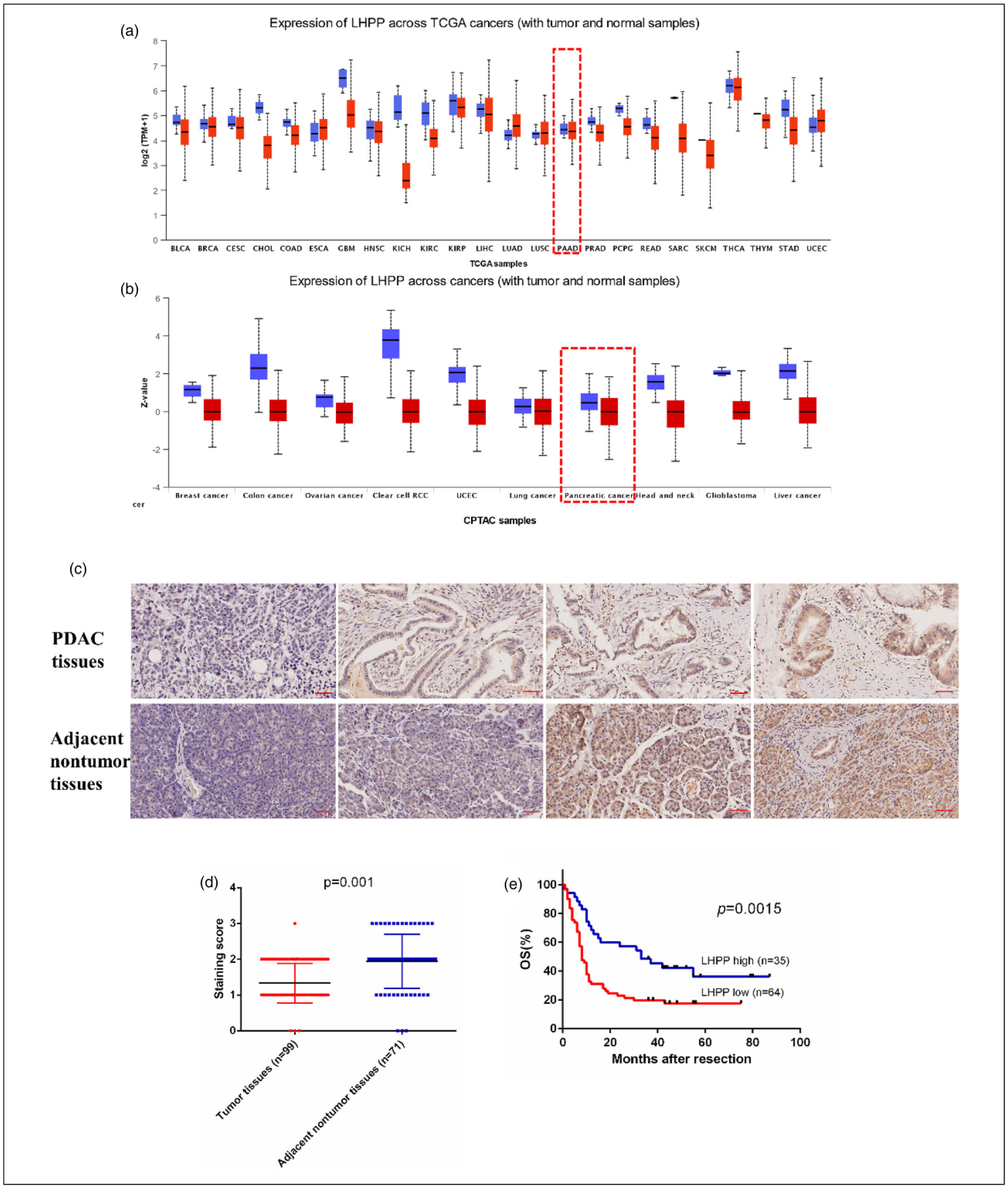

Figure 1. (a) and (b) Expression levels of LHPP in tumor and normal tissues obtained from the UALCAN database. The blue histogram represents normal tissue, and the red histogram represents tumor tissue. (c) IHC staining of LHPP in adjacent nontumor tissues and PDAC tissues, scale bar, 50 μm. (d) Staining score of LHPP in normal adjacent nontumor tissues and PDAC tissues, normal tissues (n = 99), adjacent nontumor tissues (n = 71), $P = .001$. (e) Kaplan–Meier curve analysis. A considerably longer OS was observed in the LHPP high expression group (n = 35) as compared to the LHPP low expression group (n = 64). Median OS: 33 months *versus* 8 months, $P = .0015$, log-rank test. Abbreviations: IHC, immunohistochemical; LHPP, phospholysine phosphohistidine inorganic pyrophosphate phosphatase; PDAC, pancreatic ductal adenocarcinoma; OS, overall survival.

LHPP low expression group (n = 64 patients), and the overall survival (OS) of patients in both groups was compared. Patients in the LHPP low expression group had a significantly worse prognosis, lower OS and shorter survival time compared to those in the LHPP high expression group (Figure 1e). Moreover, univariate and multivariate COX regression analyses suggested that LHPP expression level, pathological grade, and N stage were independent prognostic factors for patients with PDAC (Table 1). The clinicopathological characteristics of the patients with PDAC are listed in Supplemental Table 1.

LHPP Inhibits the Cellular Viability, Migration, and Proliferation of PDAC Cells

To investigate the specific effects of LHPP expression on PDAC progression, we used lentiviral infection to stably KD or OE LHPP in BxPC-3 and PANC-1 cells, as shown in Figure 2a and b. Subsequently, the effects of LHPP expression on the cellular viability, migration, and proliferation of these cells were detected and analyzed using CCK-8 assay, Transwell assay, and flow cytometry, respectively. The results showed that overexpression of LHPP significantly inhibited the cellular viability, migration and proliferation of BxPC-3 and PANC-1 cells, while knockdown of LHPP promoted the viability, migration, and proliferation of these cells, as shown in Figure 2c to e.

LHPP Inhibits PDAC Xenograft Tumors Growth In Vivo

The above results indicated that LHPP could inhibit the proliferation and migration of PDAC cells *in vitro*. Subsequently, the effects of LHPP OE or KD on the tumor formation and growth of PDAC cells *in vivo* were investigated using a subcutaneous xenograft mouse model. The size and weight of tumor masses formed in the OE group mice were significantly smaller than those in the NC group ($P = 0.001$), whereas the size and weight of tumor masses formed in the KD group mice were significantly larger than those in the NC group, as shown in Figure 3a to c. These results suggested that LHPP inhibited the tumor formation and growth of PDAC cells *in vivo.*

Table 1. Univariate and Multivariate Analysis of Factors Associated With the Survival of 99 Patients With PDAC.

	Survival		
	Univariate analysis *P*-value	Multivariate analysis	
		HR (95% CI)	*P*-value
Age	.815		
Gender	.624		
Pathology grade	**.006**	9.493(1.379-4.240)	**.002**
Location	.784		
T stage	.217		
N stage	**.014**	7.378(1.234-3.677)	**.007**
M stage	.439		
AJCC stage	**.020**		.723
LHPP (low vs high)	**.001**	4.023(0.318-0.987)	**.045**

Abbreviations: AJCC, American Joint Committee on Cancer;LHPP, phospholysine phosphohistidine inorganic pyrophosphate phosphatase; PDAC, pancreatic ductal adenocarcinoma.

Overexpression or Knockdown of LHPP Significantly Affects the Expression of 27 Proteins, Especially SDC1 and S100P

Given the unique role of LHPP in potentially impeding PDAC progression, we sought to explore its possible mechanism of action using proteomic analysis. TMT quantitative proteomic analysis displayed that 32 proteins were upregulated and 92 proteins were downregulated in the LHPP-KD group compared to the NC group, while 81 proteins were upregulated and 158 proteins were downregulated in the LHPP-OE group, as shown in Figure 4a. Subsequently, the differentially expressed proteins were analyzed using GO and KEGG pathway enrichment analyses, as shown in Figure 4b and c. According to the GO annotation results, the main biological processes enriched for differentially expressed proteins included "cellular processes," "metabolic processes," "biological regulation," and "response to stimulus"; the main molecular functions enriched were "binding" and "catalytic activity"; and the main cellular components enriched were "membrane" and "protein-containing complex," as shown in Figure 4b. According to the KEGG pathway analysis, the differentially expressed proteins in the KD and OE groups were mainly co-enriched in "chemical carcinogenesis," as shown in Figure 4c.

Subsequently, 30 differentially expressed proteins were screened from all the differentially expressed proteins for PRM validation. The screening criteria were as follows: (1) the proteins that were identified by both PRM and TMT; (2) the proteins with FC >1.2 or <0.833 and *P*-value <.05 compared to the NC group; (3) PRM unique peptides >2; and (4) functional proteins. Twenty-seven proteins could be accurately identified by PRM, and these proteins are listed in Table 2. In the KD group, the expression levels of IL1A, SDC1, and NAA50 were significantly upregulated, whereas the expression of L1A, THBD, ANXA6, PTMS, SPRR1B, ITGA6, ALDH1A3, DHRS1, and S100A14 were significantly downregulated. Furthermore, in the OE group, the expression levels of SCD, HSPA4L, F3, H1-5, JAG1, CDK6, HNRNPAB, and CHORDC1 were significantly upregulated, whereas the expression of DDX58, TGM2, S100P, TRIM25, NCEH1, and OAS3 were significantly downregulated (Table 2). Taking the largest expression difference and the largest number of Ingenuity Pathway Analysis (IPA) as keywords entries for the screening criteria, it was observed that the significant upregulation of SDC1 and downregulation of S100P could meet the screening criteria in the KD and OE groups, respectively. The validation results of RT-qPCR and western blot also demonstrated that both mRNA and protein levels of SDC1 were significantly upregulated in BxPC-3 and PANC-1 cells with LHPP-KD, while mRNA and protein levels of S100P were significantly

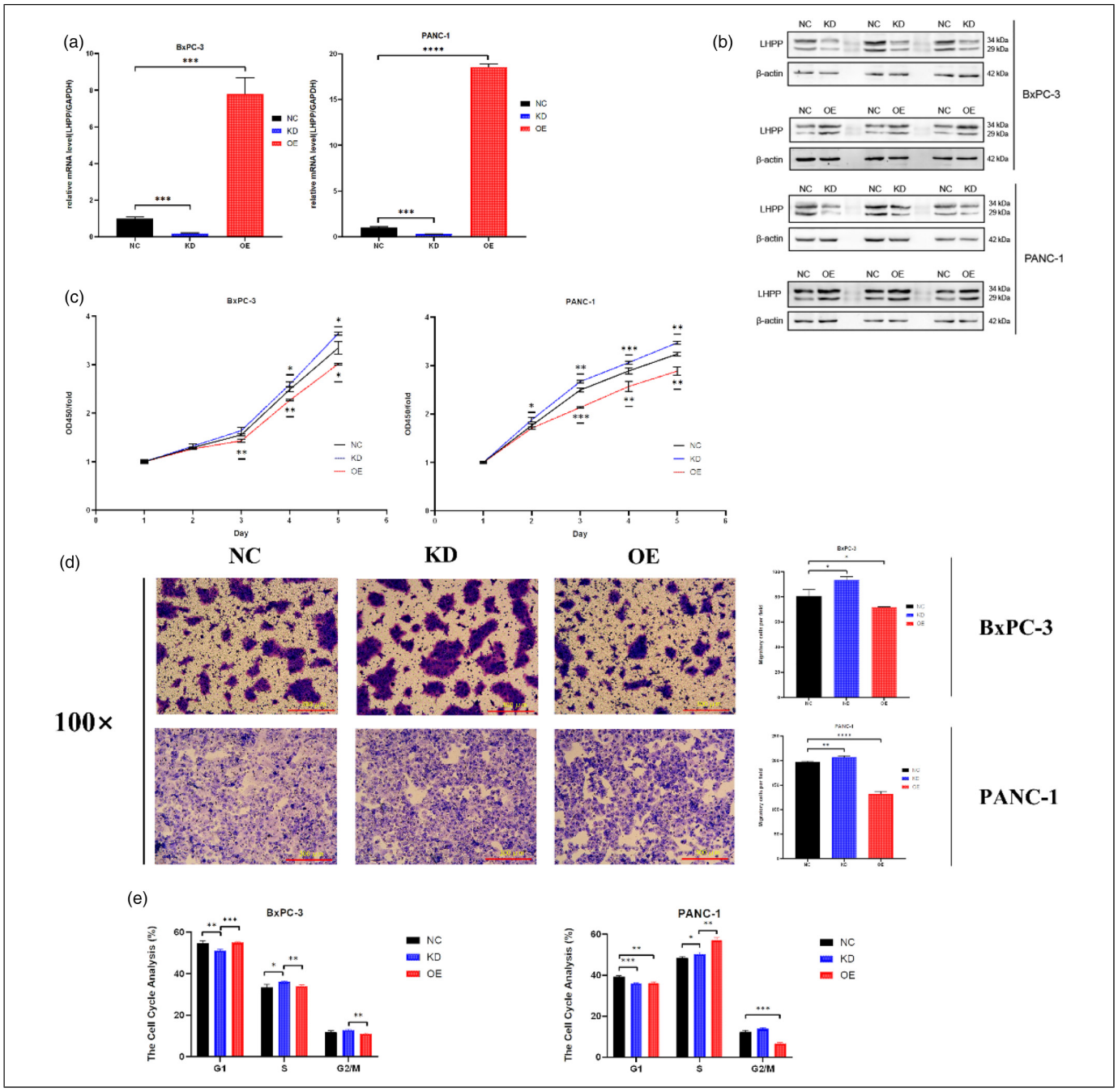

Figure 2. Overexpression and knockdown efficiencies were confirmed using qRT-PCR (a) and WB analyses (b). WB shows the results of an independent replicated experiment. However, in each of the independent replicate experiments, 3 replicates were performed for each sample. (c) Viabilities of PDAC cells with LHPP overexpressed or knocked down were analyzed using CCK-8 assay. (d) Migration abilities of PDAC cells with LHPP overexpressed or knocked down were analyzed using the Transwell assay. (e) Cellular proliferation abilities of PDAC cells with LHPP overexpressed or knocked down were analyzed using flow cytometry. $^{*}P < .05$, $^{**}P < .01$, $^{***}P < .001$, and $^{****}P < .0001$. Abbreviations: LHPP, phospholysine phosphohistidine inorganic pyrophosphate phosphatase; PDAC, pancreatic ductal adenocarcinoma; RT-qPCR, real-time quantitative polymerase chain reaction; WB, western blot.

downregulated in BxPC-3 and PANC-1 cells with LHPP-OE, as shown in Figure 5. These data suggested that LHPP KD might be involved in PDAC progression by upregulating SDC1 expression, while high expression of LHPP might by downregulating S100P expression.

Discussion

Boyer detected the intermediate product of oxidative phosphatase known as phosphohistidine, in 1962, which led to the discovery of LHPP.[19] In 2018, LHPP was first shown to be

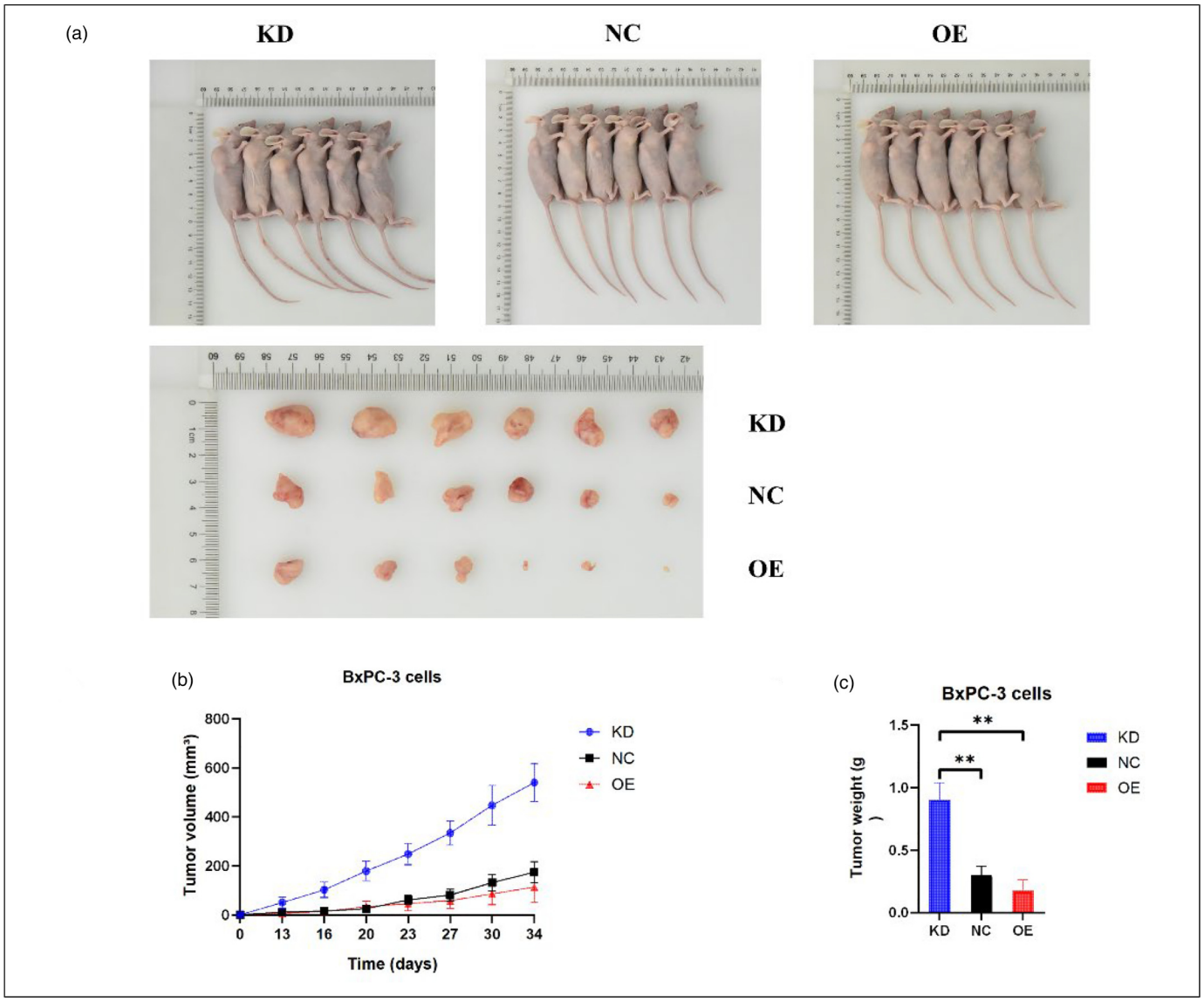

Figure 3. (a) images of xenograft tumors in the mice inoculated with stably transfected BxPC-3 cells. (b) and (c) Tumor weight and volume (g in weight and mm^3 in volume) in the NC, KD, and OE groups were quantitatively analyzed using GraphPad Prism 8 software. $^{**}P < .01$. Abbreviations: KD, knockdown; NC, normal control; OE, overexpression.

involved in cancer progression, and to be a tumor suppressor in HCC.[10] Restoration or increase of LHPP expression level can significantly delay the progression of HCC and improve the prognosis.[9,20] Recent study discovered that KD of LHPP promoted the development and metastasis of HCC, and the expression levels of LHPP were negatively correlated with the expression levels of the genes involved in epithelial-to-mesenchymal transition (EMT).[21] Subsequent successive studies have reported key antitumor roles of LHPP in different types of cancer and different mechanisms of action. In glioblastoma, LHPP might induce the ubiquitin-proteasome degradation of PKM2, thereby preventing glycolysis and respiration throughout energy metabolism and slowing tumor growth.[22] In oral squamous cell carcinoma, LHPP could inhibit tumor growth by inhibiting the PI3K/AKT signaling pathway activation and inducing apoptosis.[23] In colorectal cancer, overexpression of LHPP could lead to a significant increase in the expression level of Smad7, which negatively regulated the TGF-β/Smad signaling pathway.[24] The tumor-suppressing effects of LHPP were also observed in renal cancer and intrahepatic cholangiocarcinoma.[25,26]

In this study, *in vitro* and *in vivo* experiments demonstrated the tumor suppressive effect of LHPP in PDAC. KD of LHPP significantly promoted the proliferation and migration of PDAC cells and the growth of xenograft tumors *in vivo*. In contrast, LHPP overexpression exhibited a significant inhibitory effect on PDAC cell proliferation, migration and xenograft tumor growth *in vivo*. In addition, this study not only identified the downregulation of LHPP expression in PDAC, but also revealed the correlation between LHPP levels and prognosis

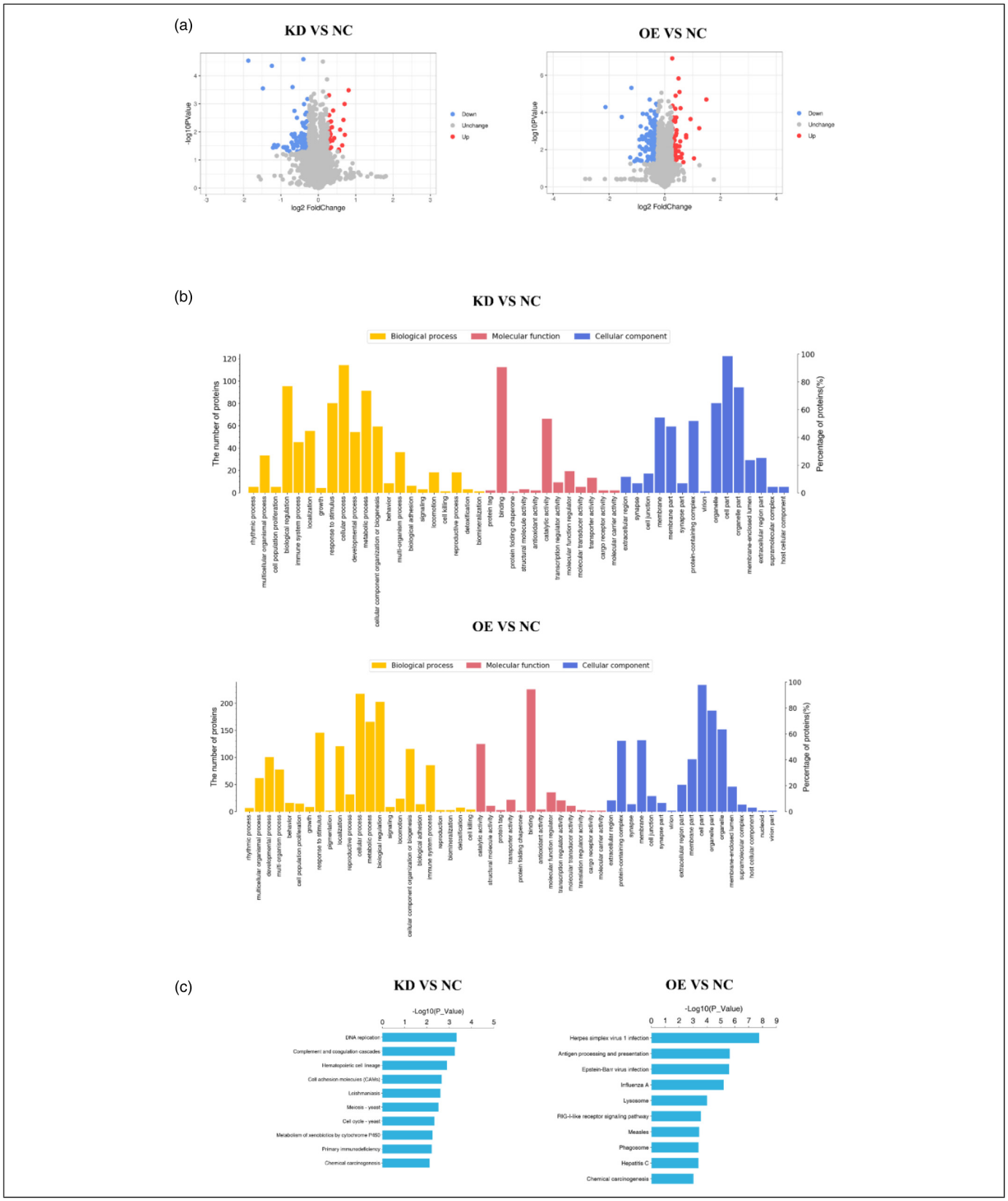

Figure 4. (a) Volcano plot. (b) Statistical histogram of significantly enriched GO terms. (c) Statistical histogram of significantly enriched KEGG pathways. Abbreviations: GO, gene ontology; KEGG, Kyoto Encyclopedia of Genes and Genomes.

Table 2. PRM Protein Quantification Results.

Protein accession	Gene name	KD/ NC	*P*-value	OE/ NC	*P*-value
O00767	SCD	0.865	3.441E-03	1.762	1.178E-03
O95757	HSPA4L	1.108	1.089E-03	1.439	2.407E-05
O95786	DDX58	0.849	4.817E-04	0.405	2.619E-06
P01583	IL1A	0.357	2.072E-04	0.722	1.949E-04
P07204	THBD	0.309	2.846E-03	0.726	1.100E-01
P08133	ANXA6	0.425	1.118E-04	0.686	5.663E-04
P13726	F3	1.042	1.255E-01	1.240	8.584E-03
P16401	H1-5	1.144	1.737E-03	1.189	7.014E-04
P17931	LGALS3	1.483	1.955E-04	0.867	2.769E-02
P18827	SDC1	1.474	2.189E-04	0.990	8.558E-01
P20962	PTMS	0.693	1.496E-02	0.687	1.239E-02
P21980	TGM2	0.757	1.595E-05	0.456	2.462E-07
P22528	SPRR1B	0.376	2.131E-03	0.624	1.319E-02
P23229	ITGA6	0.452	3.015E-06	0.988	5.703E-01
P25815	S100P	0.990	7.654E-01	0.661	4.669E-04
P47895	ALDH1A3	0.360	8.545E-08	1.132	1.747E-03
P78504	JAG1	1.008	7.458E-01	1.848	1.091E-05
Q00534	CDK6	0.769	4.082E-04	1.382	9.703E-05
Q14258	TRIM25	0.722	1.178E-03	0.650	4.520E-04
Q6PIU2	NCEH1	0.869	2.592E-04	0.575	1.116E-05
Q96LJ7	DHRS1	0.440	1.977E-05	0.697	4.062E-04
Q99729	HNRNPAB	1.262	6.469E-02	1.351	5.752E-02
Q9GZZ1	NAA50	1.330	4.289E-03	1.226	1.248E-02
Q9H008	LHPP	0.682	3.403E-01	11.766	1.458E-05
Q9HCY8	S100A14	0.623	5.412E-06	1.032	7.950E-02
Q9UHD1	CHORDC1	1.027	2.551E-01	1.355	1.133E-04
Q9Y6K5	OAS3	0.813	3.923E-01	0.174	4.879E-03

Abbreviations: KD, knockdown; NC, normal control; PRM, parallel reaction monitoring.

of patients with PDAC. Patients with high LHPP expression had significantly better prognosis. The expression level of LHPP, pathological grade, and N stage were independent prognostic factors for patients with PDAC. These data demonstrate the potential of LHPP as a prognostic predictor for PDAC and the potential of LHPP plasmids delivered by technologies such as nanoparticles for the treatment of PDAC.[27,28]

The molecular characteristics and mechanism of LHPP were investigated using proteomics analysis, and a number of proteins affected by LHPP expression were identified. According to GO annotation and KEGG enrichment, these proteins are mainly involved in cellular processes, metabolic processes, biological regulation, stimulatory responses, and even chemical carcinogenesis. These proteins may be more membrane proteins or components of protein complexes, or enzymes with catalytic activity. For example, SCD (stearoyl coenzyme A desaturase) is a key lipid regulator that may be involved in PDAC resistance to gemcitabine and cisplatin.[29] LHPP exerts its tumor suppressive effects in PDAC probably by regulating these proteins.

This study showed that the expression of SDC1 was significantly upregulated in the LHPP-knocked down BxPC-3 cells. SDC1 is a heparin sulfate proteoglycan (HSPG), belonging to the syndecan proteoglycans family. IPA keyword analysis suggests that SDC1 is a protein associated with cellular apoptosis, invasion, and proliferation. SDC1 exhibits significant pro-pathogenic effects on cancer, which can enhance the signaling of oncogenes and growth factors, prevent cancer cell death, and support angiogenesis.[30] In addition, the localization of SDC1 on the cell surface of PDAC regulates micropinocytosis, an important metabolic pathway that promotes PDAC cell

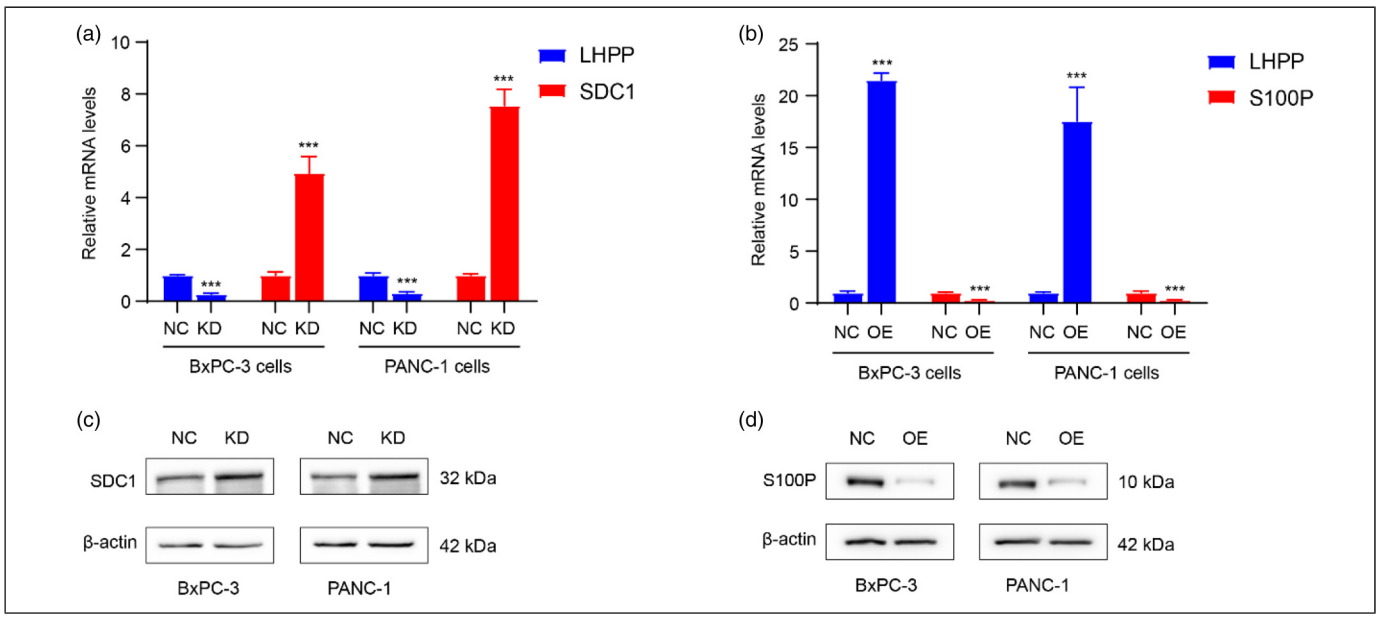

Figure 5. (a) The relative mRNA levels of SDC in BxPC-3 and PANC-1 cells that knocked down LHPP with qRT-PCR. (b) The relative mRNA levels of S100P in BxPC-3 and PANC-1 cells that overexpressed LHPP with qRT-PCR. (c) The protein expression of SDC with western blot. (d) The protein expression of S100P with western blot. $^{***}P < .001$. Abbreviations: LHPP, phospholysine phosphohistidine inorganic pyrophosphate phosphatase; RT-qPCR, real-time quantitative polymerase chain reaction; SDC, Syndecan.

growth and is critical for PDAC progression.[31] E-cadherin is a common tumor suppressor protein, and its expression is often lost in metastatic tumor cells. Another study on pancreatic cancer suggests that silencing the *SDC1* gene stimulates the production of E-cadherin.[32] Furthermore, cancer cells exhibit increased levels of E-cadherin after LHPP overexpression.[10] In conclusion, we speculate that reduced expression of LHPP may lead to the progression of PDAC by upregulating SDC1.

The current study also indicated that S100P expression was significantly downregulated in BxPC-3 cells overexpressing LHPP. S100P is a calcium-binding protein, and its high expression is associated with poor prognosis and strong invasiveness in various cancers,[33-36] and contributes to the aggressiveness of pancreatic cancer. S100P can maintain the growth and survival of pancreatic cancer cells by preventing the onset of apoptosis,[37] and can also drive cancer cell invasion and movement by regulating cytoskeletal remodeling.[38] Upregulation of S100P expression also exhibited induction of the EMT process in tumor cells.[39] Therefore, the present study speculates that high expression of LHPP may hinder PDAC progression, especially PDAC aggressiveness by downregulating S100P expression.

One of the limitations of this study is that only 2 cell lines were used. The use of additional cell lines for results validation would be beneficial to further increase the credibility of this study. In addition, although using proteomics, this study analyzed the proteins affected by LHPP when it acts, as well as the cellular processes and signaling pathways that may be involved. However, its specific mechanism of action and molecular pathways are still unknown and require more research and exploration. How LHPP regulates the expression of SDC1 and S100P is still unknown.

Conclusion

In summary, the current study revealed the potential of LHPP as a novel prognostic marker for PDAC, and demonstrated its tumor-suppressing role in PDAC. Proteomics analyses showed that the expression levels of 27 proteins, especially SDC1 and S100P, were significantly affected by LHPP overexpression or knockdown. These results might be of great significance for the subsequent deeper evaluation of LHPP molecular characteristics and mechanisms. LHPP might emerge as an important target for delaying the advancement of PDAC, thereby providing a novel therapeutic approach for the treatment of PDAC.

Contribution

ZX contributed to the conceptualization, methodology, software, investigation, formal analysis, and writing—original draft. SZ was involved in data curation; XG and HS in visualization, and investigation; FY in resources and supervision; HZ in software and validation; HG and JL in visualization and writing—review and editing; and XZ in conceptualization, funding acquisition, resources, supervision, and writing—review and editing.

Declaration of Conflicting Interests

The author(s) declared no potential conflicts of interest with respect to the research, authorship, and/or publication of this article.

Ethical Statement

The human tissue samples involved and the associated experimental plan in this study were approved by the Ethics Committee of Shandong Provincial Hospital (2020-3019; dated: December 19, 2020), and written informed consent was obtained from all included patients. The patient consented to the collection of tissue, its use in the experiments, and the publication of the results. The patients were informed about the purpose and main content of the whole study. This study does not involve any patient privacy. The animal-related experimental plan involved in this study was approved by the Ethics Committee of Shanghai Genechem Co. Ltd (GSZE0257693; dated: October 27, 2020).

Funding

The author(s) disclosed receipt of the following financial support for the research, authorship, and/or publication of this article: This work was supported by the Natural Science Foundation of Shandong Province, Clinical Medicine Technology Innovation Program of Jinan (grant number No. ZR2016HB40, No. ZR2019MH089, No. ZR2020MH259, No. ZR2020QH039, No. ZR2022MH157, No. 202019095).

ORCID iD

Xu Zhou https://orcid.org/0000-0002-3442-0711

Supplemental Material

Supplemental material for this article is available online.

References

1. Park W, Chawla A, O'Reilly EM. Pancreatic cancer: A review. *JAMA*. 2021;326:851-862. doi:10.1001/jama.2021.13027
2. Du L, Wang-Gillam A. Trends in neoadjuvant approaches in pancreatic cancer. *J Natl Compr Canc Netw*. 2017;15:1070-1077. doi:10.6004/jnccn.2017.0134
3. McGuigan A, Kelly P, Turkington RC, et al. Pancreatic cancer: A review of clinical diagnosis, epidemiology, treatment and outcomes. *World J Gastroenterol*. 2018;24:4846-4861. doi:10.3748/wjg.v24.i43.4846
4. Giannis D, Moris D, Barbas AS. Diagnostic, predictive and prognostic molecular biomarkers in pancreatic cancer: An overview for clinicians. *Cancers (Basel)*. 2021;13:1071. doi:10.3390/cancers13051071
5. Khomiak A, Brunner M, Kordes M, et al. Recent discoveries of diagnostic, prognostic and predictive biomarkers for pancreatic cancer. *Cancers (Basel)*. 2020;12(11):3234. doi:10.3390/cancers12113234
6. Kapszewicz M, Malecka-Wojciesko E. Simple serum pancreatic ductal adenocarcinoma (PDAC) protein biomarkers—is there anything in sight? *J Clin Med*. 2021;10:5463. doi:10.3390/jcm10225463
7. Kee JM, Muir TW. Chasing phosphohistidine, an elusive sibling in the phosphoamino acid family. *ACS Chem Biol*. 2012;7:44-51. doi:10.1021/cb200445w

8. Seal US, Binkley F. An inorganic pyrophosphatase of swine brain. *J Biol Chem*. 1957;228:193-199.
9. Hindupur SK, Colombi M, Fuhs SR, et al. The protein histidine phosphatase LHPP is a tumour suppressor. *Nature*. 2018;555:678-682. doi:10.1038/nature26140
10. Zheng J, Dai X, Chen H, et al. Down-regulation of LHPP in cervical cancer influences cell proliferation, metastasis and apoptosis by modulating AKT. *Biochem Biophys Res Commun*. 2018;503:1108-1114. doi:10.1016/j.bbrc.2018.06.127
11. Li Y, Zhang X, Zhou X, et al. LHPP suppresses bladder cancer cell proliferation and growth via inactivating AKT/p65 signaling pathway. *Biosci Rep*. 2019;39(7):BSR20182270. doi:10.1042/BSR20182270
12. Hou B, Li W, Li J, et al. Tumor suppressor LHPP regulates the proliferation of colorectal cancer cells via the PI3 K/AKT pathway. *Oncol Rep*. 2020;43:536-548. doi:10.3892/or.2019.7442
13. Sun W, Qian K, Guo K, et al. LHPP inhibits cell growth and migration and triggers autophagy in papillary thyroid cancer by regulating the AKT/AMPK/mTOR signaling pathway. *Acta Biochim Biophys Sin (Shanghai)*. 2020;52:382-389. doi:10.1093/abbs/gmaa015
14. Percie du Sert N, Hurst V, Ahluwalia A, et al. The ARRIVE guidelines 2.0: Updated guidelines for reporting animal research. *PLoS Biol*. 2020;18:e3000410. doi:10.1371/journal.pbio.3000410
15. Garber JC, Wayne Barbee R, Bielitzki JT, et al. *Guide for the Care and Use of Laboratory Animals*. 8th ed. 2011.
16. Chandrashekar DS, Karthikeyan SK, Korla PK, et al. UALCAN: An update to the integrated cancer data analysis platform. *Neoplasia*. 2022;25:18-27. doi:10.1016/j.neo.2022.01.001
17. Gene Ontology C. Gene ontology consortium: Going forward. *Nucleic Acids Res*. 2015;43:D1049-D1056. doi:10.1093/nar/gku1179
18. Kanehisa M, Goto S. KEGG: Kyoto encyclopedia of genes and genomes. *Nucleic Acids Res*. 2000;28:27-30. doi:10.1093/nar/28.1.27
19. Boyer PD, Deluca M, Ebner KE, et al. Identification of phosphohistidine in digests from a probable intermediate of oxidative phosphorylation. *J Biol Chem*. 1962;237:PC3306-PC3308.
20. Liao L, Duan D, Liu Y, et al. LHPP Inhibits hepatocellular carcinoma cell growth and metastasis. *Cell Cycle*. 2020;19:1846-1854. doi:10.1080/15384101.2020.1783472
21. Ma L, Sun H, Xu X, et al. Tumor suppressor LHPP suppresses cell proliferation and epithelial-mesenchymal transition in hepatocellular carcinoma cell lines. *J Physiol Biochem*. 2022;78(4):807-817. doi: 10.1007/s13105-022-00903-7.
22. Chen WJ, Chen LH, Wang J, et al. LHPP Impedes energy metabolism by inducing ubiquitin-mediated degradation of PKM2 in glioblastoma. *Am J Cancer Res*. 2021;11:1369-1390.
23. Liu S, Gao W, Lu Y, et al. As a novel tumor suppressor, LHPP promotes apoptosis by inhibiting the PI3 K/AKT signaling pathway in oral squamous cell carcinoma. *Int J Biol Sci*. 2022;18:491-506. doi:10.7150/ijbs.66841
24. Hou B, Li W, Xia P, et al. LHPP suppresses colorectal cancer cell migration and invasion in vitro and in vivo by inhibiting Smad3 phosphorylation in the TGF-beta pathway. *Cell Death Discov*. 2021;7:273. doi:10.1038/s41420-021-00657-z
25. Wang D, Ning Z, Zhu Z, et al. LHPP suppresses tumorigenesis of intrahepatic cholangiocarcinoma by inhibiting the TGFbeta/smad signaling pathway. *Int J Biochem Cell Biol*. 2021;132:105845. doi:10.1016/j.biocel.2020.105845
26. Zhang X, Kang H, Xiao J, et al. LHPP inhibits the proliferation and metastasis of renal cell carcinoma. *Biomed Res Int*. 2020;2020:1-9. doi:10.1155/2020/7020924
27. Wu F, Ma H, Wang X, et al. The histidine phosphatase LHPP: An emerging player in cancer. *Cell Cycle*. 2022;21:1140-1152. doi:10.1080/15384101.2022.2044148
28. Zhang Q, Xiong M, Liu J, et al. Targeted nanoparticle-mediated LHPP for melanoma treatment. *Int J Nanomedicine*. 2019;14:3455-3468. doi:10.2147/IJN.S196374
29. Wu C, Hu B, Wang L, et al. Assessment of stromal SCD-induced drug resistance of PDAC using 3D-printed zPDX model chips. *iScience*. 2023;26:105723. doi:10.1016/j.isci.2022.105723
30. Teng YH, Aquino RS, Park PW. Molecular functions of syndecan-1 in disease. *Matrix Biol*. 2012;31:3-16. doi:10.1016/j.matbio.2011.10.001
31. Yao W, Rose JL, Wang W, et al. Syndecan 1 is a critical mediator of macropinocytosis in pancreatic cancer. *Nature*. 2019;568:410-414. doi:10.1038/s41586-019-1062-1
32. Yang Y, Tao X, Li CB, et al. MicroRNA-494 acts as a tumor suppressor in pancreatic cancer, inhibiting epithelial-mesenchymal transition, migration and invasion by binding to SDC1. *Int J Oncol*. 2018;53:1204-1214. doi:10.3892/ijo.2018.4445
33. Wu Z, Boonmars T, Nagano I, et al. Significance of S100P as a biomarker in diagnosis, prognosis and therapy of opisthorchiasis-associated cholangiocarcinoma. *Int J Cancer*. 2016;138:396-408. doi:10.1002/ijc.29721
34. Wang X, Tian T, Li X, et al. High expression of S100P is associated with unfavorable prognosis and tumor progression in patients with epithelial ovarian cancer. *Am J Cancer Res*. 2015;5:2409-2421.
35. Lin M, Fang Y, Li Z, et al. S100p contributes to promoter demethylation and transcriptional activation of SLC2A5 to promote metastasis in colorectal cancer. *Br J Cancer*. 2021;125:734-747. doi:10.1038/s41416-021-01306-z
36. Kikuchi K, McNamara KM, Miki Y, et al. S100p and Ezrin promote trans-endothelial migration of triple negative breast cancer cells. *Cell Oncol (Dordr)*. 2019;42:67-80. doi:10.1007/s13402-018-0408-2
37. Arumugam T, Simeone DM, Van Golen K, et al. S100p promotes pancreatic cancer growth, survival, and invasion. *Clin Cancer Res*. 2005;11:5356-5364. doi:10.1158/1078-0432.CCR-05-0092
38. Whiteman HJ, Weeks ME, Dowen SE, et al. The role of S100P in the invasion of pancreatic cancer cells is mediated through cytoskeletal changes and regulation of cathepsin D. *Cancer Res*. 2007;67:8633-8642. doi:10.1158/0008-5472.CAN-07-0545
39. Shen Q, Zheng G, Zhou Y, et al. CircRNA circ_0092314 induces epithelial-mesenchymal transition of pancreatic cancer cells via elevating the expression of S100P by sponging miR-671. *Front Oncol*. 2021;11:675442. doi:10.3389/fonc.2021.675442